Journal of Power Sources 196 (2011) 6419–6424

Contents lists available at ScienceDirect

Journal of Power Sources

journal homepage: www.elsevier.com/locate/jpowsour

Charge–discharge rate of spinel lithium manganese oxide and olivine lithium iron phosphate in ionic liquid-based electrolytes

Minato Egashira*, Akinori Kanetomo, Nobuko Yoshimoto, Masayuki Morita

Graduate School of Science and Engineering, Yamaguchi University Tokiwadai, 2-16-1, Tokiwadai, Ube, Yamaguchi 755-8611, Japan

ARTICLE INFO

Article history:
Received 16 December 2010
Received in revised form 15 March 2011
Accepted 28 March 2011
Available online 5 April 2011

Keywords:
Lithium batteries
Ionic liquid
Spinel manganese
Olivine iron phosphate

ABSTRACT

Rate capability of Li/spinel $LiMn_2O_4$ or olivine $LiFePO_4$ positive electrode cells containing mixed imidazolium ionic liquids electrolytes has been investigated under comparison with conventional organic solvent electrolyte and piperidinium ionic liquid. The $LiMn_2O_4$ electrode provides variation of rate capabilities among the ionic liquid electrolytes, while ionic liquid electrolytes provide similar extent of capacity degradation under high rate compared with organic solvent electrolyte for $LiFePO_4$ electrode. Such differences in electrolyte dependences of the rate capabilities can be explained in relation to parameters in the high frequency resistances on AC impedance, assumed as interfacial resistances. The rate capability of $LiMn_2O_4$ is somewhat related to the activation energy of the high frequency resistance, while for $LiFePO_4$ the resistance value appears to contribute to the rate capability.

1. Introduction

Ionic liquids have been attracted as candidates of non-flammable electrolyte of lithium batteries [1–28]. Many studies have been conducted for the evaluation of test cells containing electrolytes containing many kinds of ionic liquids and many types of negative/positive electrodes. While the intensive studies by Matsumoto et al. in order to obtain sufficient rate capabilities from battery cells containing ionic liquids electrolytes by using the ones based on bis(fluorosulfonyl)imide (FSI) anion [16], in most cases their rate capabilities are poorer than those containing conventional organic solvent electrolytes. Such poor rate capabilities are one of the major reasons why ionic liquid electrolytes are not presently applied in practical lithium battery cells.

As larger current flows, a battery cell exhibits larger extent of capacity degradation caused by internal resistances in the cell. All conduction processes must include resistances, and the sole internal resistance of a cell is the combination of these fractions. Therefore, the rate capability of a cell is influenced by all components and all conduction processes. In the cases of ionic liquid electrolytes, the dominant factor for the rate capability of the cell is assumed to be the ion conduction resistance in bulk electrolytes and the interfacial resistance between viscous ionic liquids and porous electrodes [16,29,30]. These resistance fractions can be minimized by the modification of the cell manufacturing. On the other hand, it is impossible to remove charge-transfer resistances between electrodes and electrolyte because this fraction is intrinsic for charge–discharge reactions in batteries. Recent studies reveal that the charge-transfer process concerted with ion intercalation includes rate determination step of de-solvation of solvated mineral ion [31,32]. According to this study, the rate of electrode/electrolyte surface processes of a cell can be influenced by the kind of electrolyte at some extent.

The authors have proposed new types of ionic liquids and mixed ionic liquids based on 1,3-substituted imidazolium cation for the use in lithium batteries. It has been widely known that ionic liquids having 1-ethyl-3-methyl imidazolium (EMI), while their excellent fluidities, suffer from their low stabilities at negative electrode potential. In contrast, ionic liquid based on 1-cyanomethyl-3-methyl imidazolium (CmMI) cation provides rather stable cycling of lithium deposition/dissolution, an analogue for negative electrode reaction, by providing surface protective film on lithium surface [33]. The performance of positive electrodes such as $LiMn_2O_4$ and $LiFePO_4$, and hard carbon negative electrode was previous reported under constant low current conditions [34]. A purpose of this study is to confirm the properties, in particular the rate capabilities, of positive electrodes $LiMn_2O_4$ and $LiFePO_4$ in the mixed ionic liquid electrolytes containing EMI and CmMI cations. In addition, the contribution of the surface charge-transfer process on the rate capability of the electrodes in ionic liquid-based electrolytes has also been discussed. Such properties in the EMI–CmMI mixed ionic liquid electrolytes have been compared with the case of ionic liquid electrolyte based on N-methyl-N-propyl piperidinium (PP13) cation and a typical organic solvent electrolyte ethylene carbonate

* Corresponding author. Tel.: +81 836 85 9212; fax: +81 836 85 9201.
E-mail address: minato@yamaguchi-u.ac.jp (M. Egashira).

0378-7753/$ – see front matter © 2011 Elsevier B.V. All rights reserved.
doi:10.1016/j.jpowsour.2011.03.075

(EC)-diethyl carbonate (DEC) containing 0.8 mol dm^{-3} of $LiPF_6$. The properties of two kinds of positive electrodes, spinel $LiMn_2O_4$ and olivine $LiFePO_4$, are also compared in the various electrolytes.

2. Experimental

An active material of positive electrode, $LiMn_2O_4$ (Toda Kogyo Co., Japan) or $LiFePO_4$ (acquired from Hohsen Co., Japan) was mixed with acetylene black and poly(vinylidene difluoride) (PVdF; Kureha Chemical Co., Japan) binder as the gravimetric ratio of active material:AB:PVdF was 8:1:1 in 2-methylpirrolidinone (NMP) solvent. The resulting slurry was spread onto an aluminum foil, dried at 120 °C under vacuum, and then composite electrode sheet was obtained. The loading amount of active material in a coin cell was controlled to ca. 1.7 mg and the electrode thickness was ca 50 μm.

Imidazlium ionic liquids with bis(trifluoromethanesulfone)imide (TFSI) anion, EMITFSI and CmMITFSI, were kindly provided by Nippon Synthtic Chemical Industry Co., Japan. PP13TFSI (Kanto Chemical Co., Japan) was used for comparison. These ionic liquids were used after vacuum drying at 120 °C overnight. The ionic liquid electrolytes with the molar ratio of LiTFSI:EMITFSI:CmMITFSI became 2:7:1 or 2:6:2 and LiTFSI:PP13TFSI ratio became 2:8 were prepared. Hereafter these electrolytes are denoted as Li:EMI:CmMI = 2:7:1, Li:EMI:CmMI = 2:6:2, and PP13, respectively. These molar ratio of EMI:CmMI were determined from the balance between the viscosity and the reversibility of lithium deposition–dissolution in these solutions, as discussed precisely at ref. [33]. The conductivites at 25 °C of Li:EMI:CmMI = 2:7:1, Li:EMI:CmMI = 2:6:2 are 2.9 and 2.2 mS cm^{-1}, respectively. These viscosities at room temperature are 68 and 154 cP, respectively.

A 2032 stainless-steel coin cell was assembled with test electrode above, lithium metal (0.25 mm in thickness and 12 mm in diameter, Honjo Metal Co., Japan) counter electrode, electrolyte and separator (Celgard 2501). The LiTFSI/ionic liquid electrolytes described above, and the electrolyte solution of 0.8 mol dm^{-3} $LiPF_6$ in the mixed solvent of ethylene carbonate (EC) and diethyl carbonate (DEC) (denoted as EC:DEC) were used here. Charge–discharge tests of the two-electrode cells under constant-current conditions were conducted with a cycle test apparatus (BTS2004, Nagano Co., Japan). The cut-off voltages were from 3.5 V to 4.6 V for $LiMn_2O_4$, from 2.5 V to 3.8 V for $LiFePO_4$, under prescribed current density. These measurements were conducted at room temperature.

The resistances between electrolyte and a positive electrode were monitored by AC impedance measurement. A three-electrode sealed cell with stainless-steel body (Hohsen Co., Japan) was assembled with lithium foils at reference and counter electrodes. Similar composite electrode sheets to coin cell tests were used as working electrode. The cell was cycled once in order to check the performance of the cell, and then potentiostatically polarized at a prescribed potential. After the applied current became negligible, the AC polarization was carried out around the potential with the bias of 10 mV and the frequency range from 2×10^5 to 10^{-3} Hz. For the DC and AC polarization same apparatus (Solartron 1260) was used. The cell temperature was controlled during DC and AC polarization by a temperature chamber (SU-241, Espec Co., Japan). The impedance data were fitted into adequate RC circuits by using a program in Z-plot software.

3. Results and discussion

3.1. Performance of positive electrodes in ionic liquid electrolytes

Fig. 1 summarizes typical constant-current charge–discharge behavior in an initial cycle of (a) $LiMn_2O_4$ and (b) $LiFePO_4$ in such electrolytes as EC:DEC, PP13, and EMI–CmMI mixed ionic liquid electrolytes under the current density of 0.02 mA cm^{-2}. Both $LiMn_2O_4$ and $LiFePO_4$ positive electrodes exhibit charge–discharge plateau around 4 V and 3.5 V, respectively in the all electrolyte used here, with significant overvoltage in the ionic liquid electrolytes. Except for $LiMn_2O_4$ in Li:EMI:CmMI = 2:7:1, the discharge capacities of both electrodes in the ionic liquid electrolytes were lower than those in EC:DEC electrolytes. From Fig. 1(a), the order of the electrolytes by the discharge capacities of $LiMn_2O_4$ is EC:DEC > Li:EMI:CmMI = 2:7:1 > Li:EMI:CmMI = 2:6:2 > PP13. This order is somewhat resemble to the order of viscosity, EC:DEC < Li:EMI:CmMI = 2:7:1 < Li:EMI:CmMI = 2:6:2 < PP13. This tendency suggests that the relatively low capacities in the ionic liquid electrolytes are the result of the low level of electrolyte immersion into porous electrode. The ionic liquid electrolytes with high viscosity is resistive for the immersion into interparticlar pores of the composite electrode, resulting to reduce effective area of electrode/electrolyte interface and also effective mass of electrode. The $LiMn_2O_4$ case appears to meet this explanation. For the $LiFePO_4$ case, the order of ionic liquid electrolytes is different from the $LiMn_2O_4$ case. The capacities of $LiFePO_4$ in the EMI–CmMI mixed electrolytes are lower than expected, and the increase of the content of the CmMI ionic liquid appears to reduce the capacity.

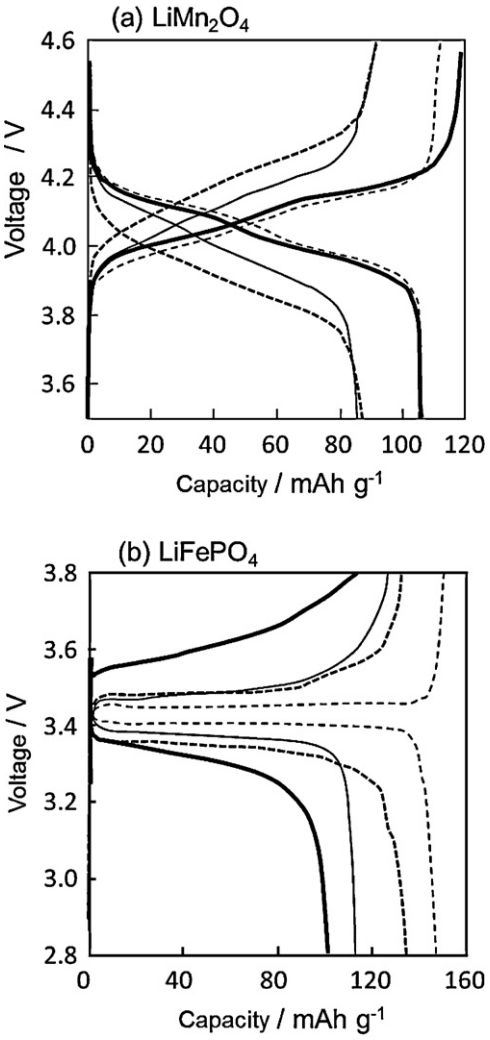

Fig. 1. Constant-current charge–discharge profiles of positive electrodes in various electrolytes. Electrode: (a) $LiMn_2O_4$, (b) $LiFePO_4$. Electrolyte: (thin broken line) EC:DEC, (thick solid line) Li:EMI:CmMI = 2:7:1, (thin solid line) Li:EMI:CmMI = 2:6:2, (thick broken line) PP13. Current density: 0.02 mA cm^{-2}, cut-off: (a) 3.0–4.5 V vs. Li/Li^+, (b) 3.0–4.0 V vs. Li/Li^+.

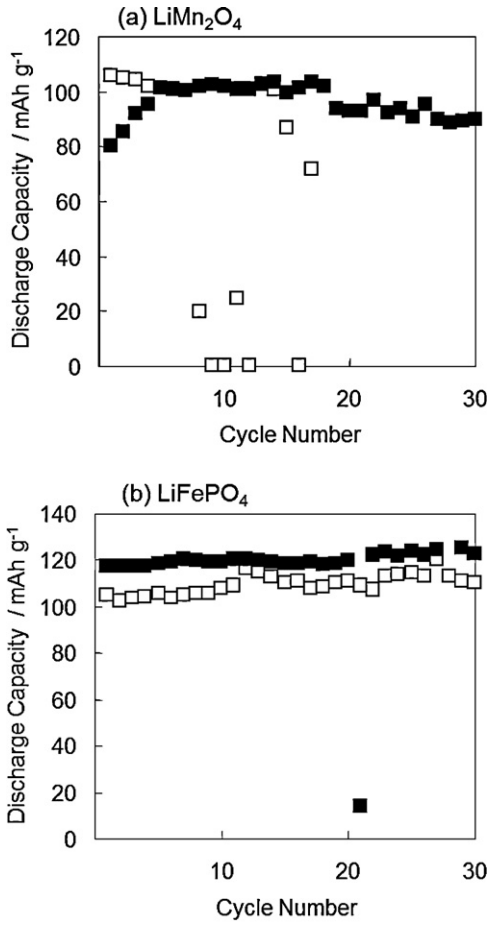

Fig. 2. Plots of discharge capacities toward cycles in various electrolytes. Electrode: (a) $LiMn_2O_4$, (b) $LiFePO_4$. Electrolyte: (open squere) Li:EMI:CmMI = 2:7:1, (closed square) Li:EMI:CmMI = 2:6:2. Current density: 0.02 mA cm^{-2}, cut-off: (a) 3.0–4.5 V vs. Li/Li$^+$, (b) 3.0–4.0 V vs. Li/Li$^+$.

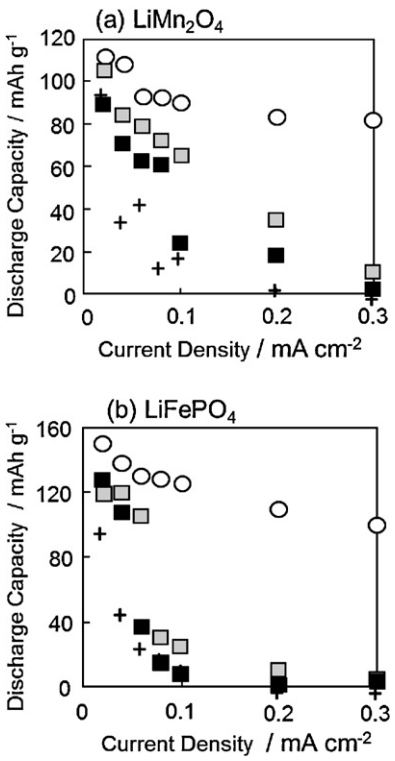

Fig. 3. Rate dependences of capacities in various electrolytes. Electrode: (a) $LiMn_2O_4$, (b) $LiFePO_4$. Electrolyte: ○ EC:DEC, □ Li:EMI:CmMI = 2:7:1, ■ Li:EMI:CmMI = 2:6:2, +PP13. Cut-off: (a) 3.0–4.5 V vs. Li/Li$^+$, (b) 3.0–4.0 V vs. Li/Li$^+$.

This tendency indicates that the EMI–CmMI mixed systems are more resistive than the PP13 system by other reason than the viscosity. The authors have previously revealed that the CmMI ionic liquid has rather 'polar' property because of the polarized electronic structure of CmMI cation [35]. Such an electronic structure may provide different wettability toward $LiFePO_4$ electrode which increases the resistance for electrolyte immersion. $LiFePO_4$ may be coated by carbon and causes the repulsive interaction toward the EMI–CmMI mixed ionic liquids.

Fig. 2 shows the plots of discharge capacities of (a) $LiMn_2O_4$ and (b) $LiFePO_4$ in Li:EMI:CmMI mixed ionic liquid electrolytes under the current density of 0.02 mA cm^{-2}. During initial 30 cycles, the capacities of both electrodes remains, that is, the charge–discharge reactions of these positive electrodes are occurred reversibly even in imidazolium-based mixed ionic liquid electrolytes, expect of $LiMn_2O_4$ in Li:EMI:CmMI = 2:7:1 electrolyte, which exhibits capacity degradation after 10 cycles. From the comparison with the behavior of $LiFePO_4$, the capacity degradation of $LiMn_2O_4$ in Li:EMI:CmMI = 2:7:1 electrolyte might be due to the slow anodic decomposition of EMI fraction in the mixed electrolyte. Another possibility lies on the influence of cathodic decomposition product on the positive electrode side. It is to be noted that the CmMI content of 10 mol% is not sufficient for prolonged lithium deposition–dissolution cycles [33], even though the excess amount of lithium counter electrode may assure stable charge–discharge in initial cycles. In both the mixed electrolytes, the capacity of $LiMn_2O_4$ in the mixed electrolytes gradually increases during initial several cycles, while that of $LiFePO_4$ increases slightly during 30 cycles. Such capacity increases may be due to the immersion of electrolyte into pores of electrode.

The dependences of charge–discharge current densities on the specific capacities of both electrodes are summarized in Fig. 3. Under the current density of 0.3 mA cm^{-2}, approximately corresponding to 1.6C for $LiMn_2O_4$ and 1.1C for $LiFePO_4$, the specific capacities of both electrodes in the EC:DEC electrolyte are ca. 70% of those under the current density of 0.02 mA cm^{-2}. In contrast, the capacities in the ionic liquid electrolytes fade by the increase of current density at 0.3 mA cm^{-2} while both electrodes exhibit similar capacities in these ionic liquid electrolytes to the EC:DEC electrolyte under 0.02 mA cm^{-2}. The precise comparison of the rate dependences for both electrodes in the ionic liquid electrolyte exhibits the difference of the extent of the capacity degradation by the electrode and ionic liquid electrolyte. In the current range between 0.03 and 0.2 mA cm^{-2}, the capacities of $LiMn_2O_4$ in the Li:EMI:CmMI mixed ionic liquid systems are significantly larger than that in PP13 system. At the current density of 0.08 mA cm^{-2}, the ratios of capacities of $LiMn_2O_4$ in Li:EMI:CmMI = 2:7:1, Li:EMI:CmMI = 2:6:2, and PP13 to that in EC:DEC are 0.78, 0.67, and 0.17, respectively. For the case of current density of 0.2 mA cm^{-2}, the capacities are 0.42, 0.24, 0.07, respectively. In contrast, $LiFePO_4$ exhibits similar capacity degradation in the current range regardless of the composition of the ionic liquid electrolytes: the ratios of capacities to that in EC:DEC at 0.08 mA cm^{-2} are below 0.25, and those are nearly zero at the current density of 0.2 mA cm^{-2}. Such capacity fades are significantly different from the values for $LiMn_2O_4$. For the both positive electrode, the test cells were same size coin cell and the test electrode sheets had similar configurations. Therefore the difference in the rate behavior by using different ionic liquid electrolyte must be mainly due to the interfacial resistance between ionic liquid electrolyte and electrode. In order to estimate the difference of interfacial resistance between various electrolyte and both elec-

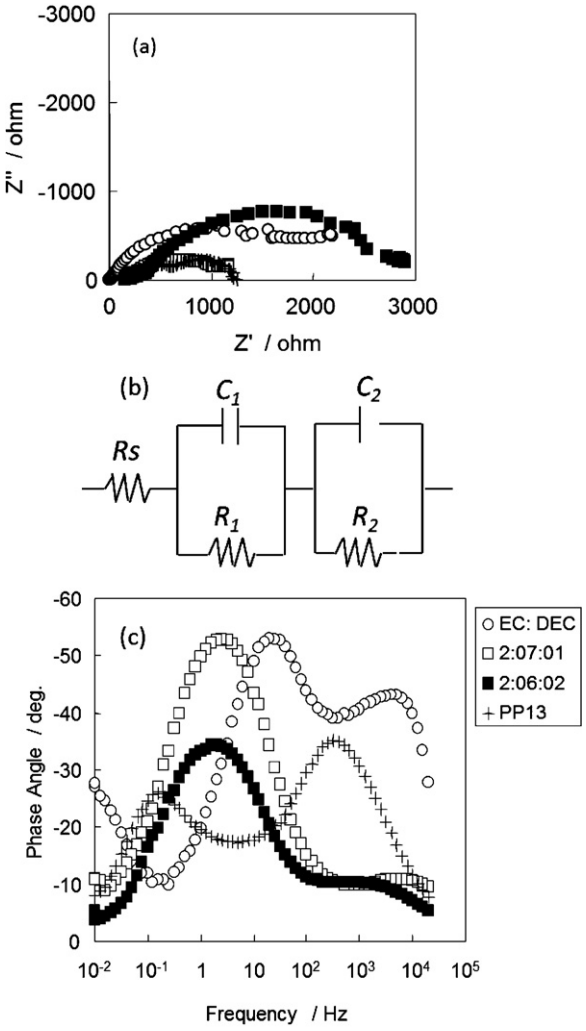

Fig. 4. AC impedance diagrams of $LiMn_2O_4$ electrode in various electrolytes at 3.9 V, 25 °C. (a) Nyquist plots, (b) equivalent circuit, (c) Bode plots. Electrolyte: ○ EC:DEC, □ Li:EMI:CmMI = 2:7:1, ■ Li:EMI:CmMI = 2:6:2, +PP13.

trodes, AC impedance measurements were conducted using the three-electrode test cell.

3.2. Interfacial resistance of positive electrodes/ionic liquid electrolytes

The Nyquist plots of $LiMn_2O_4$ electrodes charged at 3.9 V in various electrolytes at 25 °C are shown in Fig. 4(a). For all cases one or two semicircles, indicating the existence of RC parallel fractions in equivalent circuit as shown in Fig. 4(b), are observable while the diameter of semicircles, the resistance values in RC fractions, are different by the kind of electrolyte. When two RC fractions having different resistance values are connected in series, the existence of the smaller semicircle is difficult to be distinguished from the larger one. In order to clarify the existence of RC fractions, the frequency dependence of phase angle, that is Bode plots, are also referred. The Bode plots for the cases of Fig. 4(a) are shown in Fig 4(c). In such Bode plots, the existence of RC fractions is indicated as a peak. It is clear that two RC parallel fractions are included in all the systems of the interface between $LiMn_2O_4$ electrode and electrolytes shown in the figure. In each case one peak are around 10^{-1} to 10^2 Hz and the other lies above 10^2 Hz. Similar impedance measurements were carried out at various electrode potentials and various temperatures. The resistance values of the both the former

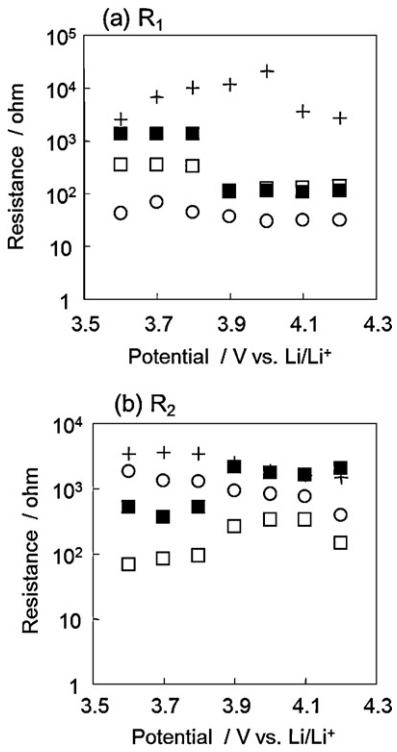

Fig. 5. Dependences of resistance fractions on the state of charge of $LiMn_2O_4$ in various electrolytes at 25 °C. (a) R_1, (b) R_2. Electrolyte: ○ EC:DEC, □ Li:EMI:CmMI = 2:7:1, ■ Li:EMI:CmMI = 2:6:2, +PP13.

(later denoted as R_1) and the latter (denoted as R_2) RC fractions at the interface between $LiMn_2O_4$ and various electrolytes measured at 25 °C are plotted versus its potential in Fig. 5(a) and (b), respectively. The R_1 decreases in the potential range from 3.8 to 3.9 V for the electrolytes except for PP13 in which R_1 decreases at 4.1 V, while the R_2 are rather independent of electrolyte type and the potential of $LiMn_2O_4$. The decrease of R_1 by the increase of the electrode potential implies that this fraction indicates the charge-transfer process at electrode–electrolyte interface. Xia et al. claimed that such impedance of $LiMn_2O_4$ electrode exhibits two resistance fractions with different frequencies which are assigned to the process concerning a surface film on $LiMn_2O_4$ at higher frequencies [36]. In the case of the present study, the resistances of both surface film and charge-transfer may be included in R_1. The behaviors of R_2 are somewhat complicated and at the present state there is no information which identifies the origin of R_2, while this is considered to be from macroscopic phenomenon. Here the R_1 at various temperatures are collected in various electrolytes and compared under the basis of Arrhenius manner.

Fig. 6 shows the Arrhenius plots of the reciprocal of R_1 in various electrolyte-$LiMn_2O_4$ systems. The R_1 values are varied by the kind of electrolyte. The EC:DEC electrolyte provides lower R_1 than the ionic liquid electrolytes, while these values are closer at high temperature. Among the cases of the ionic liquid electrolytes, the R_1 in Li:EMI:CmMI = 2:6:2 electrolyte is significantly lower. The plots roughly exhibit Arrhenius-type temperature dependences. The disturbance in particular found at 55 °C may be due to the influence of the dissolution of manganese from $LiMn_2O_4$. Due to such disturbances, it is difficult to acquire activation energies which have sufficient correctness for rigorous quantitative discussion. The approximate values of activation energies estimated from the data under 45 °C are 15, 29, 56, and 55 kJ mol^{-1} for the cases in EC:DEC, Li:EMI:CmMI = 2:7:1, 2:6:2, and PP13 electrolytes, respectively. All values are ranged in 15–60 kJ mol^{-1} and at similar extent

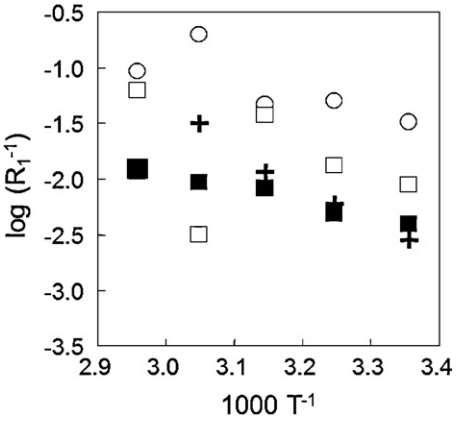

Fig. 6. Arrhenius plots of inverse R_1 value of $LiMn_2O_4$ at 4.2 V in various electrolytes. Electrolyte: ○ EC: □ DEC, Li:EMI:CmMI = 2:7:1, ■ Li:EMI:CmMI = 2:6:2, +PP13.

to the activation energies of lithium intercalation reported previously [31,32]. When compared with each electrolyte, the order of activation energy appears to be somewhat related to that of capacity duration at high rate charge–discharge. Since the order between the intrinsic activation energy in Li:EMI:CmMI = 2:6:2 and that in PP13 is not distinguishable due to the scattering of Arrhenius plots, the order of the activation energy can be written as: EC + DEC < Li:EMI:CmMI = 2:7:1 < (Li:EMI:CmMI = 2:6:2, PP13). This order appears to be similar to that of the electrolyte by the rate capabilities of $LiMn_2O_4$

Similar impedance measurements and analyses are also carried out for the case of $LiFePO_4$ electrode. The Nyquist plots, Bode plots at 25 °C and at 3.8 V vs. Li/Li$^+$, and the Arrhenius plots of the interfacial resistances, the fraction between 10 and 10^4 Hz, at 3.8 V, are shown in Fig. 7(a), (b) and (c), respectively. Also in this case, Bode plots indicate that the existence of two RC parallel fractions in all electrolyte. However, the existence of low frequency resistance in the EC:DEC electrolyte is suspicious from corresponding Nyquist plot. Therefore in this case the fraction between 10 and 10^4 Hz is assumed as the interfacial resistance and denoted as R_1. The feature of Arrhenius plots in the ionic liquid electrolytes compared with that in EC:DEC is different from the case of $LiMn_2O_4$. In the case of this electrode, the interfacial resistance values in the ionic liquid electrolytes are at similar extent and far larger than those in EC; DEC. The activation energies for $LiFePO_4$ in EC:DEC, Li:EMI:CmMI = 2:7:1, 2:6:2, and PP13 are estimated to 36, 78, 40, and 57 kJ mol^{-1}, respectively. The activation energies in the ionic liquid electrolytes are varied with electrolytes also in the case of $LiFePO_4$ electrode. From such tendency, it is suggested that apparent pre-exponential factor in interfacial resistances, likely including the effect of surface lithium concentration, mainly contribute to the rate capability of $LiFePO_4$ more largely than the activation energy.

The behavior at the interface between the ionic liquid electrolyte and a positive electrode clearly depends on the kind of positive electrode, while the extent of activation energies are rather similar and in the range between 15 and 78 kJ mol^{-1} regardless of the kind of electrode and electrolyte. According to the previous studies by Yamada et al. [31,32], the rate determination step for intercalation processes of lithium ion is its de-solvation. On the basis of this finding, the activation energies of R_1 for $LiMn_2O_4$ and $LiFePO_4$ in a given electrolyte must be similar. However, the activation energy values of R_1 for $LiMn_2O_4$ and $LiFePO_4$ are different for some cases. For the interface at $LiMn_2O_4$, the contribution of surface film may be included in the interfacial resistance fraction. While the existence and functions of surface films by organic solvent electrolytes have been reported, it has still been unclear whether the existence of similar surface film also in ionic liquid electrolytes. These results

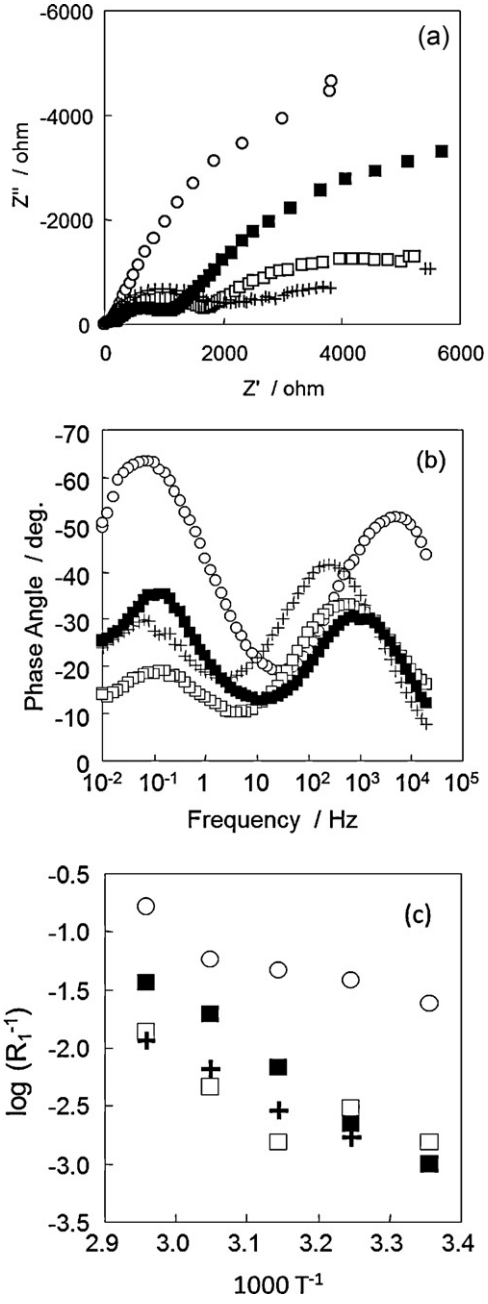

Fig. 7. (a) Nyquist and (b) Bode plots of $LiFePO_4$ in various electrolytes at 3.8 V, 25 °C. (c) Arrhenius plots of inverse R_1 values of $LiFePO_4$ at 3.8 V in various electrolytes. Electrolyte: ○ EC: □ DEC, Li:EMI:CmMI = 2:7:1, ■ Li:EMI:CmMI = 2:6:2, +PP13.

support the existence of similar surface film to organic solvent electrolyte, which controls the rate of the surface process. Based on this assumption, the Li:EMI:CmMI mixed ionic liquid electrolytes are considered to provide more compact surface films on $LiMn_2O_4$ compared with the PP13 electrolyte. The existence of surface film may also affect the difference of contribution of surface reaction rates on the charge–discharge rate capabilities of $LiMn_2O_4$ from $LiFePO_4$. While the CmMI ionic liquid provides an effective surface film on lithium metal electrode [33,37], in this case it is unclear which component contributes to form such good film on $LiMn_2O_4$. It is our future trial to display direct evidences of the presence of such surface film in ionic liquid electrolyte, non-volatile nature of which prevents them to be removed out by 'washing' procedure as frequently used for organic solvent electrolyte.

4. Conclusion

Spinel manganese oxide $LiMn_2O_4$ electrode exhibits different rate behaviors by the electrolyte used, while the rate capabilities of olivine iron phosphate $LiFePO_4$ in the ionic liquid electrolytes are similarly poor compared with that in a conventional organic solvent electrolyte. The mixed imidazolium ionic liquid electrolytes containing cyanomethyl derivative provides better rate capabilities of $LiMn_2O_4$ than piperidinium ionic liquid. The variation of the rate of surface process between $LiMn_2O_4$ and electrolyte appears to contribute to such difference in the rate capabilities. The present study reveals that such electrodes as $LiMn_2O_4$ provide possibility of improved rate capabilities in the ethylmethyl and cyanomethyl methyl mixed imidazolium ionic liquid electrolytes by the modification of cell configuration.

Acknowledgements

The present work is financially supported by NEDO (New Energy and Development Organization). The authors thank to Nippon Synthetic Chemical Industry Co. for providing high purity EMITFSI and CmMITFSI ionic liquids.

References

[1] N. Koura, K. Iizuka, Y. Idemoto, K. Ui, Electrochemistry 67 (1999) 706.
[2] Y.S. Fung, R.Q. Zhou, J. Power Sources 81–82 (1999) 891.
[3] H. Nakagawa, S. Izuchi, K. Kuwana, T. Nukuda, Y. Aihara, J. Electrochem. Soc. 150 (2003) A695.
[4] Y. Katayama, M. Yukumoto, T. Miura, Electrochem. Solid-State Lett. 6 (2003) A96.
[5] H. Matsumoto, H. Sakaebe, Electrochem. Commun. 5 (2003) 594.
[6] P.C. Howlett, D.R. MacFarlane, A.F. Hollenkamp, Electrochem. Solid-State Lett. 7 (2004) A97.
[7] B. Garcia, S. Lavallée, G. Perron, C. Michot, M. Armand, Electrochim. Acta 49 (2004) 4583.
[8] M. Egashira, S. Okada, J. Yamaki, D.A. Dri, F. Bonadies, B. Scrosati, J. Power Sources 138 (2004) 240.
[9] T. Sato, T. Maruo, S. Marukane, K. Takagi, J. Power Sources 138 (2004) 253.
[10] H. Matsumoto, H. Sakaebe, J. Tatsumi, Power Sources 146 (2005) 45.
[11] K. Hayashi, Y. Nemoto, K. Akuto, Y. Sakurai, J. Power Sources 146 (2005) 689.
[12] H. Zheng, J. Qin, Y. Zhao, T. Abe, Z. Ogumi, Solid State Ionics 176 (2005) 2219.
[13] A. Chagnes, M. Diaw, B. Carré, P. Willmann, D. Lemordant, J. Power Sources 145 (2005) 82.
[14] E. Markevich, V. Baranchugov, D. Aurbach, Electrochem. Commun. 8 (2006) 1331.
[15] S. Seki, Y. Kobayashi, H. Miyashiro, Y. Ohno, A. Usami, Y. Mita, N. Kihara, M. Watanabe, N. Terada, J. Phys. Chem. B 110 (2006) 10228.
[16] H. Matsumoto, H. Sakaebe, K. Tatsumi, M. Kikuta, E. Ishiko, M. Kono, J. Power Sources 160 (2006) 1308.
[17] M. Egashira, M. Tanaka-Nakagawa, I. Watanabe, S. Okada, J. Yamaki, J. Power Sources 160 (2006) 1387.
[18] H. Zheng, B. Li, Y. Fu, T. Abe, Z. Ogumi, Electrochim. Acta 52 (2006) 1556.
[19] M. Ishikawa, T. Sugimoto, M. Kikuta, E. Ishiko, M. Kono, J. Power Sources 162 (2006) 658.
[20] A. Fernicola, F. Croce, B. Scrosati, T. Watanabe, H. Ohno, J. Power Sources 174 (2007) 342.
[21] K. Tsunashima, F. Yonekawa, M. Sugiya, Chem. Lett. 37 (2008) 314.
[22] S. Seki, Y. Ohno, H. Miyashiro, Y. Kobayashi, A. Usami, Y. Mita, N. Terada, K. Hayamizu, S. Tsuzuki, M. Watanabe, J. Electrochem. Soc. 155 (2008) A421.
[23] A. Guefi, S. Duchesne, Y. Kobayashi, A. Vijh, K. Zaghib, J. Power Sources 175 (2008) 866.
[24] T. Sugimoto, Y. Atsumi, M. Kikuta, E. Ishiko, M. Kono, M. Ishikawa, J. Power Sources 189 (2009) 802.
[25] H. Saruwatari, T. Kuboki, T. Kishi, S. Mikoshiba, N. Takami, J. Power Sources 195 (2010) 1495.
[26] S. Seki, T. Kobayashi, N. Serizawa, Y. Kobayashi, K. Takei, H. Miyashiro, K. Hayamizu, S. Tsuzuki, T. Mitsugi, Y. Umebayashi, M. Watanabe, J. Power Sources 195 (2010) 6207.
[27] B.S. Lalia, N. Yoshimoto, M. Egashira, M. Morita, J. Power Sources 195 (2010) 7426.
[28] J.-K. Kim, A. Matic, J.-H. Ahn, P. Jacobsson, J. Power Sources 195 (2010) 7639.
[29] C.S. Stefan, D. Lemordant, B. Claude-Montigny, D. Violleau, J. Power Sources 189 (2009) 1174.
[30] N. Tachikawa, J.-W. Park, K. Yoshida, T. Tamura, K. Dokko, M. Watanabe, Electrochemistry 78 (2010) 349.
[31] Y. Yamada, Y. Iriyama, T. Abe, Z. Ogumi, Langmuir 25 (2009) 12766.
[32] Y. Yamada, F. Sagane, Y. Iriyama, T. Abe, Z. Ogumi, J. Phys. Chem. C 113 (2009) 14528.
[33] M. Egashira, H. Todo, N. Yoshimoto, M. Morita, J. Yamaki, J. Power Sources 174 (2007) 560.
[34] M. Egashira, A. Kanetomo, N. Yoshimoto, M. Morita, Electrochemistry 78 (2010) 370.
[35] M. Egashira, M. Sumimoto, N. Yoshimoto, M. Morita, K. Hori, Electrochemistry 77 (2009) 237.
[36] Y. Xia, Y. Zhou, M. Yoshio, J. Electrochem. Soc. 144 (1997) 2593.
[37] L. Zhao, J. Yamaki, M. Egashira, J. Power Sources 174 (2007) 352.